Journal of Statistical Physics, Vol. 62, Nos. 5/6, 1991

Lorentz Lattice Gases, Abnormal Diffusion, and Polymer Statistics

X. P. Kong[1] and E. G. D. Cohen[1]

Received November 13, 1989; final March 27, 1990

Diffusive behavior in various Lorentz lattice gases, especially wind-tree-like models, is discussed. Comparisons between lattice and continuum models as well as deterministic and probabilistic models are made. In one deterministic model, where the scatterers behave like double-sided mirrors, a new kind of abnormal diffusion is found, viz., the mean square displacement is proportional to the time, but the probability density distribution function is non-Gaussian. The connections of this mirror model with the percolation problem and the statistics of polymer chains on a lattice are also discussed.

KEY WORDS: Lorentz model; Ehrenfest wind-tree model; lattice gas; diffusion; abnormal diffusion; bond percolation; polymer chain.

1. INTRODUCTION

In Lorentz gases independent point particles move through randomly placed stationary scatterers. These systems are named after H. A. Lorentz,[1] who first introduced them as a model to study the electrical conductivity of metals. Here identical hard spherical objects elastically scatter oncoming particles (cf. Fig. 1a). Subsequently, the Ehrenfests[2] introduced the so-called wind-tree model to illuminate some of the difficulties in understanding the nature of the *Stoszzahl Ansatz* in the Boltzmann equation. In this case diamonds (trees) with parallel corresponding diagonals scatter onrushing (wind) particles (cf. Fig. 1b) in the plane. While in the case of spherical scatterers all velocity directions can occur, in the wind-tree model, only four occur if a (wind) particle starts out in one of the four directions along the $\pm x$ or $\pm y$ axes. In all Lorentz models there is only one conserved quantity in a collision with a scatterer: the

[1] Rockefeller University, New York, New York 10021.

0022-4715/91/0300-1153$06.50/0

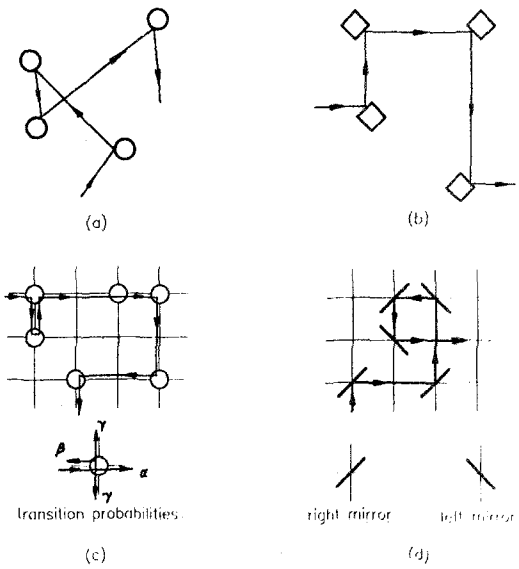

Fig. 1. Particle trajectories in various Lorentz models: (a) circular Lorentz model; (b) Ehrenfest wind-tree model; (c) probabilistic lattice Lorentz model with transition probabilities shown (for clarity, the trajectory of the particle has been drawn slightly away from the lattice); (d) mirror model with both kinds of mirrors shown.

number of particles. The momentum of a particle is not conserved and its energy is trivially connected with its mass, since the speed v of each particle never changes and only a redistribution of velocity directions occurs. Therefore, in Lorentz gases one considers diffusion processes rather than the flow processes that occur in fluids where mutually interacting particles move together.

In a normal diffusion process, the probability $P(\mathbf{r}, t)$ to find a particle at the position $\mathbf{r}$ at time t obeys the diffusion equation

$$\frac{\partial P(\mathbf{r}, t)}{\partial t} = D \nabla^2 P(\mathbf{r}, t) \tag{1.1}$$

where D is the diffusion coefficient. The solution of Eq. (1.1) is a Gaussian:

$$P(\mathbf{r}, t) = \left[\frac{1}{4\pi D t}\right]^{d/2} e^{-r^2/4Dt} \tag{1.2}$$

if the particle is initially at the origin at $t = 0$. Here d is the dimension of space and $r = |\mathbf{r}|$. From (1.2) it follows immediately that for a normal

diffusion process the mean square displacement $\Delta(t)$ is proportional to the time t:

$$\Delta(t) = \langle r^2 \rangle = 2dDt \tag{1.3}$$

or

$$\langle x^2 \rangle = 2Dt \tag{1.3'}$$

Here the average is over initial distributions of the scatterers. For a Gaussian distribution function of $\vec{r}$, all odd moments in $\mathbf{r}$ vanish, while all even moments can be expressed in terms of the second moment, so that all (even) cumulants vanish. In particular, the kurtosis

$$K = \frac{\langle x^4 \rangle - 3\langle x^2 \rangle^2}{\langle x^2 \rangle^2} \tag{1.4}$$

vanishes.

The only quantity left to be determined is the diffusion constant D, which can be achieved by kinetic theory. In particular, one can then determine the dependence of D on the density n of the scatterers. In the next section we will summarize some kinetic theory results for a number of Lorentz models with different scatterers, in particular for the continuum Ehrenfest wind-tree model.

2. KINETIC THEORY FOR CONTINUUM LORENTZ MODELS

2.1. Low-Density Limit

In this case the diffusion coefficient D can be computed from a linear Boltzmann equation.[3] This equation only takes into account "uncorrelated collisions," where the wind particle never scatters twice from the same scatterer, so that no memory effects are taken into account. Then one has for spherical scatterers of radius a,[3]

$$D^{\text{sph}} = \frac{v}{3\pi n a^2} \xrightarrow{a=v=1} \frac{1}{3\pi n} \tag{2.1a}$$

for disks of radius a,[3]

$$D^{\text{disk}} = \frac{3v}{16na} \xrightarrow{a=v=1} \frac{3}{16n} \tag{2.1b}$$

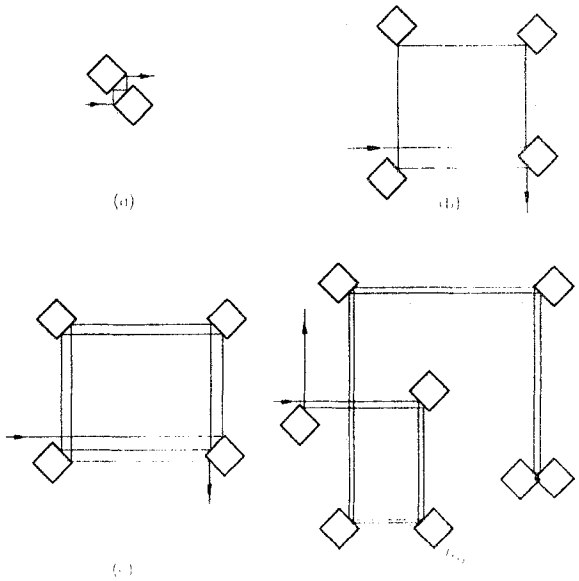

Fig. 2. Four kinds of events which contribute to the corrections to the Boltzmann approximation of the diffusion coefficient of the Ehrenfest wind-tree model: (a) repeated collisions between two scatterers; (b) ring events; (c) orbiting events; (d) retracting events. For definitions of these events, see ref. 4.

and for the wind-tree model,[3]

$$D^{\text{w.t.}} = \frac{v}{4na} \xrightarrow{a=v=1} \frac{1}{4n} \tag{2.1c}$$

where a is the length of half of a diagonal in the case of the wind-tree model. In this paper we will use units throughout such that $a = v = 1$.

2.2. Intermediate Density

In this case corrections to the Boltzmann approximation have to be taken into account that incorporate correlations between collisions when scatterers are hit more than once by a wind particle. To obtain the first correction to the Boltzmann result for the wind-tree model, i.e., the term of $O(1)$ in the density n, one has to consider four classes of events, typical examples of which are sketched in Fig. 2. The contributions of these events to D were computed by Hauge and Cohen[4,7] for two cases:

2.2.1. NOV Case. The scatterers (trees) cannot overlap. Then one finds

$$D^{\text{w.t.}} = D_B^{\text{w.t.}} + D_{\text{corr}}^{\text{w.t.}} \tag{2.2a}$$

where

$$D_{\text{corr}}^{\text{w.t.}} = -\left\{\frac{\pi^2+41}{72} + \frac{1}{3\pi} + (<0.1)\right\} \tag{2.2b}$$

and the expectation is that a normal diffusion process takes place.

2.2.2. OV Case. The scatterers can overlap each other. In that case an abnormal diffusion process occurs, slower than normal, since the mean square displacement $\Delta(t)$ grows slower than t,[4,5]

$$\Delta(t) \sim t^{1\ \ 4n/3 + O(n^2)} \sim D(t)t \tag{2.3}$$

This behavior is due to the retracing events (cf. Fig. 2), which cause excessive backscattering of the wind particles. From (2.3) and (1.3) it follows that the diffusion coefficient defined by

$$D = \lim_{t \to \infty} D(t) = 0 \tag{2.4}$$

vanishes in this case.

These results for D were confirmed by computer simulations of Wood and Lado[6] (cf. Fig. 3). In view of the developments discussed below, a determination of $P(\mathbf{r}, t)$ would be of interest. This behavior of the diffusion

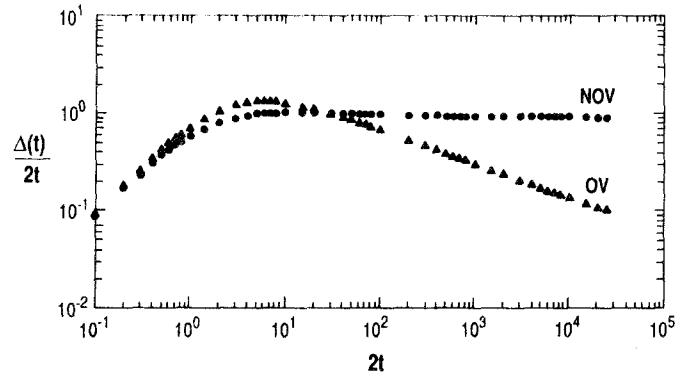

Fig. 3. Normal and abnormal diffusion in the Ehrenfest wind-tree model with 8192 scatterers (from ref. 6).

in the OV case only obtains for $n < 1$ approximately. For high n, a dynamical phase transition occurs,[5,7,8] to a phase where no diffusion takes place anymore, since a wind particle finds itself always trapped, due to a percolation transition of the trees.

3. THE LORENTZ LATTICE GASES

In the Lorentz lattice gas, independent point particles move in discrete (unit) time steps on a discrete regular lattice from site to site, a number of which are occupied randomly by stationary scatterers (cf. Fig. 1c). We will restrict ourselves to a square lattice and consider two types of scattering laws:

(i) Probabilistic: such models have been extensively studied by Binder, Ernst, and van Velzen.[9-12] Here the probabilities for particle to be scattered upon collision in the forward (α), backward (β), or side direction (γ) are given (cf. Fig. 1c). Clearly, $\alpha + \beta + 2\gamma = 1$ must be satisfied. The case $\alpha = \beta = 0$, $\gamma = 1/2$ appears to correspond to the continuous wind-tree model.

(ii) Deterministic: we will discuss a strictly deterministic model, introduced by Ruijgrok and Cohen,[13] where the scatterers behave like double-sided mirrors that are oriented along the diagonals of the lattice at angles $+\pi/4$ (right mirror) or $-\pi/4$ (left mirror) with the positive x axis, respectively (cf. Fig. 1d).

Two mirror models have been considered: model A, where the mirrors are fixed, and model B, where they flip to the other direction after collision. Hence, in model B, there are interactions between the moving particles via the mirrors. The case of equal nuumbers of left and right mirrors seems to correspond to the wind-tree model. Thus, in the probabilistic models there are two types of lattice sites: with or without a scatterer; while in the deterministic mirror model there are three types: with a right, a left, or no mirror.

4. PROBABILISTIC MODELS

To treat these models, we introduce occupation variables $c_{\mathbf{n}}$ such that $c_{\mathbf{n}}$ equals 1 or 0, depending on whether the site $\mathbf{n} = (n_x, n_y)$ is or is not occupied by a scatterer, respectively. In the Boltzmann approximation of uncorrelated collisions, one replaces all $c_{\mathbf{n}}$ by c, the fraction of the lattice sites occupied by scatterers. This implies that one then replaces the set of occupied and unoccupied lattice sites, characterized by $\{c_{\mathbf{n}}\}$, by a "mean field approximation," where each lattice site has scattering probability $c\alpha$,

$c\beta$, $c\gamma$. As shown by Ernst and van Velzen,[12] the diffusion coefficient is then given by

$$D_B^{\text{prob}} = \frac{1}{4c(\beta+\gamma)} - \frac{1}{4} \tag{4.1}$$

where the second term on the right-hand site is due to the discreteness of the lattice,[14] and one has taken $a = v = 1$.

Two cases have to be distinguished:

(i) No reflection: $\beta = 0$. Then

$$D_B^{\text{prob}} = \frac{1}{4c\gamma} - \frac{1}{4} \xrightarrow{\alpha = 0} D_B^{\text{prob}} = \frac{1}{2c} - \frac{1}{4} \tag{4.2}$$

In this case it is believed that D_B^{prob} is the low-density limit of D, i.e., that $cD_B = \lim_{c \to 0} cD(c)$.

(ii) Reflection: $\beta \neq 0$. Then the Boltzmann expression (4.2) is not the correct low-density limit of $D(c)$, since there are contributions from correlated collisions that are of the same order in c as the uncorrelated collisions taken into account in D_B, i.e., of order c^{-1}. To account for those, the actual $\{c_n\}$ are needed. The collision events that now contribute are given in Fig. 4 and their contributions to $D(c)$ can be approximately computed using the effective medium approximation (EMA).[11,12] Figure 5 shows a comparison of $cD(c)$ as obtained from computer simulations for various probabilistic models and those in the Boltzmann and EMA approximations. The agreement of the experimental and EMA results is clearly very good.

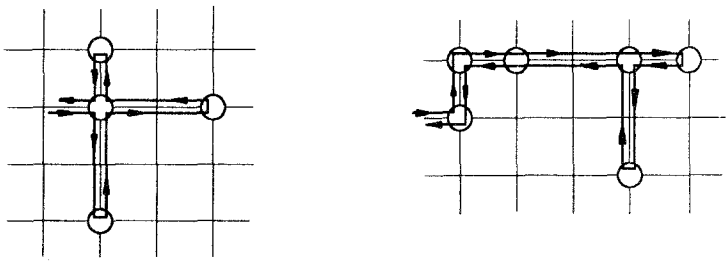

Fig. 4. Examples of events that contribute to the diffusion coefficient in order $O(1)$: (a) repeated rings; (b) nested rings. For deefinitions of these events, see refs. 11 and 12.

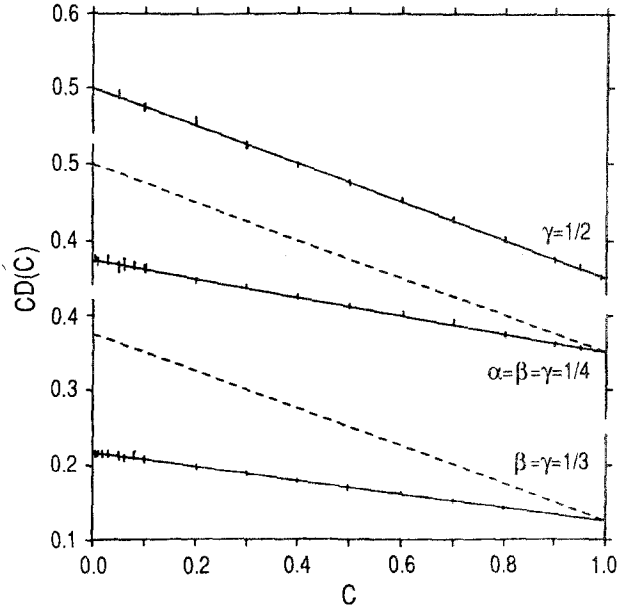

Fig. 5. Comparison of the EMA results (solid curves) for $cD(c)$ of the probabilistic Lorentz lattice model with both the Boltzmann approximation (dashed lines) and the simulation results. Simulations are indicated by their error bars only (from ref. 12).

5. MIRROR MODEL

5.1. Boltzmann Approximation

We introduce now six occupation variables:

$n_i(\mathbf{r}, t) = 1$ or 0 $(i = 1,..., 4)$, if a particle is or is not at $\mathbf{r}$, t, respectively;

$m_R(\mathbf{r}, t) = 1$ or 0, if a right mirror is or is not at $\mathbf{r}$, t, respectively;

$m_L(\mathbf{r}, t) = 1$ or 0, if a left mirror is or is not at $\mathbf{r}$, t, respectively

The microscopic equations of motion are

$$n_i(\mathbf{r} + \mathbf{e}_i, t+1) = (1 - m_R - m_L)n_i + m_R n_{i+1} + m_L n_{i-1} \qquad (i = 1, 3) \tag{5.1a}$$

$$n_i(\mathbf{r} + \mathbf{e}_i, t+1) = (1 - m_R - m_L)n_i + m_R n_{i-1} + m_L n_{i+1} \qquad (i = 2, 4) \tag{5.1b}$$

where the occupation numbers on the right-hand sides are all taken at $\mathbf{r}$, t.

To obtain the Boltzmann approximation, we proceed in two steps: first one introduces average occupation numbers f_i, defined by

$$f_i(\mathbf{r}, t) = \langle n_i(\mathbf{r}, t) \rangle \qquad (i = 1, 2, 3, 4) \tag{5.2}$$

where the average is taken over random initial configurations of the scatterers.

Second, one makes the "molecular chaos" assumption of the independence of the occupation numbers for particle velocities and mirrors on all lattice sites, i.e., one sets

$$\langle m_R n_i \rangle = \langle m_R \rangle \cdot \langle n_i \rangle = c_R \cdot f_i \qquad (i = 1, 2, 3, 4) \tag{5.3a}$$

$$\langle m_L n_i \rangle = \langle m_L \rangle \cdot \langle n_i \rangle = c_L \cdot f_i \qquad (i = 1, 2, 3, 4) \tag{5.3b}$$

where c_R and c_L are the fractions of the right and left mirrors on the lattice, respectively.

Using (5.2) and (5.3) in (5.1), one obtains the linear Boltzmann equation:

$$f_i(\mathbf{r} + \mathbf{e}_i, t + 1) = f_i(\mathbf{r}, t) + \sum_{j=1}^{4} T_{ij} f_j(\mathbf{r}, t) \qquad (i = 1, 2, 3, 4) \tag{5.4}$$

where the collision matrix is given by

$$T = \begin{pmatrix} -c & c_R & 0 & c_L \\ c_R & -c & c_L & 0 \\ 0 & c_L & -c & c_R \\ c_L & 0 & c_R & -c \end{pmatrix} \tag{5.5}$$

Solving this equation for the diffusion coefficient by either the Chapman–Enskog method[3] or the method given in ref. 10 leads to the following expression for a typical diffusion coefficient in the Boltzmann approximation when $c_R = c_L = c/2$:

$$D_B^M(c) = \frac{1}{2c} - \frac{1}{4} \tag{5.6}$$

which is the same as for the probabilistic $\gamma = 1/2$ case. For $c_L \neq c_R$, we have a diffusion tensor, with an xx or yy component equal to

$$D_B^M(c) = \frac{c}{8c_L c_R} - \frac{1}{4} \tag{5.7}$$

5.2. Computer Simulations

We checked the above results on a Microvax II, using a 1024×1024 basic lattice with periodic boundary conditions for the scatterers. About 2600 particles were randomly distributed among the lattice sites and their motion was followed on the infinite checkerboard formed by the basic lattice and its periodic images, for typically time steps up to several thousand mean free times, where the mean free time equals $1/c$ here. For $\Delta(t)$ and D an average was taken over about 20 different random configurations of the scatterers after an average had been obtained over the 2600 particles in each configuration. However, for the probability density distribution functions more elaborate averages were needed in order to obtain sufficiently accurate representations of these functions. Thus, in that case first an average was taken over a group of 100 different random configurations of the scatterers as well as over the 2600 particles in each configuration; then a second average was carried out over ten such groups. The statistical errors (standard deviation of the mean) are given in the figure captions; for the mirror models, the error bars are always within the symbols used in the figures. We first quote the results for model A.

5.2.1. Model A. (i) Mean square displacement. The diffusion coefficients, defined in Eq. (1.3), are plotted for several mirror concentrations in Fig. 6. They reach constant values in the large time limit.[13,14] $cD(c)$ is plotted as a function of c for $c_R = c_L = c/2$ in Fig. 7. The positive deviations from the Boltzmann result, Eq. (5.6), can amount to about 17%. They can be ascribed to local fluctuations in the random mirror distribu-

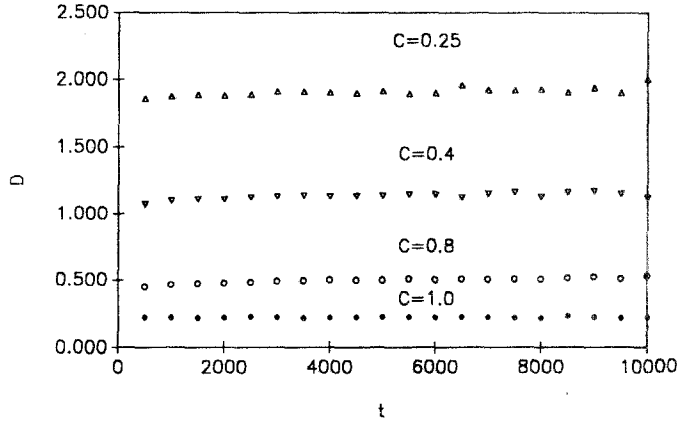

Fig. 6. Time dependence of D of the fixed mirror model for several concentrations. Each data point was averaged over 20 configurations and the statistical error is ~ 0.03 for $c = 0.25$, ~ 0.02 for $c = 0.4$, and ~ 0.01 for $c = 0.8$ and 1.0.

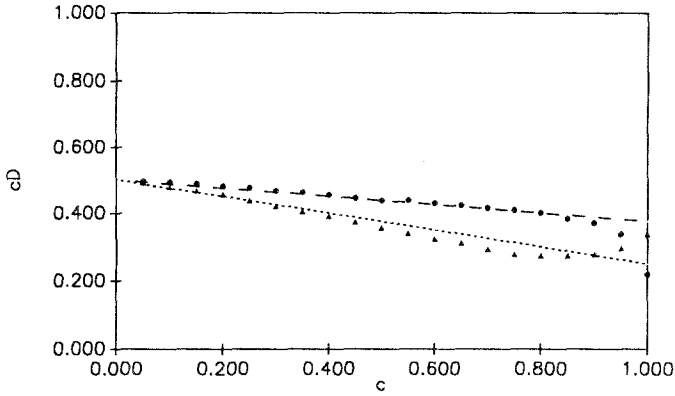

Fig. 7. Concentration dependence of $cD(c)$ of the fixed mirror model (filled circles) and flipping mirror model (filled triangles) at $t = 4000$ time steps. The dotted line is the Boltzmann approximation and the dashed line is the equation $cD = cD_B + c/8$. Each data point was averaged over ten configurations for the flipping mirror model and 50 for the fixed mirror model; the statistical error for both curves is ~ 0.004.

tion leading to patches of parallel (either right or left) mirrors that speed up the diffusion due to zigzag motions. The experimental points are fitted well by the formula[14] $cD = cD_B + c/8$ for $0 < c < 0.8$. The sharp decrease of D for $c \geqslant 0.8$ can be related to the quickly increasing probability of closed orbits which slow down the diffusion.

(ii) Kurtosis. Except for very low density, the kurtosis (cf. Fig. 8) is manifestly different from zero, leading to a maximum of about 3.7 for

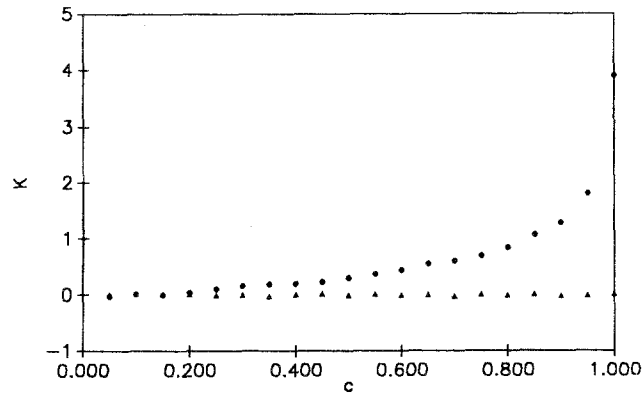

Fig. 8. Concentration dependence of the kurtosis of the fixed (filled circles) and the flipping (filed triangles) mirror models at $t = 400$ time steps. The configurations used here were the same as in Fig. 7 and the statistical error is ~ 0.06 for the fixed mirror model and 0.03 for the flipping mirror model.

$c_R = c_L$ and $c = 1$. This implies a non-Gaussian density distribution function $P(\mathbf{r}, t)$, in spite of the proportionality of $\Delta(t)$ with t.

(iii) Probability density distribution function. We computed the distribution function $\hat{P}(r, t) = 2\pi r P(r, t)$, the probability density of finding a particle between a distance r and $r + dr$ at t if it was at the origin at $t = 0$.

In Fig. 9, $\hat{P}(r, t)$ is plotted for four concentrations at $t = 1024$. The jumping of the experimental data with increasing steps of r reflects the difference in the number of trajectories on which a particle can reach neighboring points. For all c there is a sharp maximum near the origin, which increases with c, due to the increasing probability that a particle, starting at the origin, will find itself in a closed orbit when the number of scatterers increases. For intermediate r, there is a depletion of probability as compared to a Gaussian P, while for large r there is an excess of probability compared to the Gaussian P, which could be related to the diminished probability of a particle to be in a closed orbit and the effect of zigzags. In Fig. 10 the time evolution of $\hat{P}(r, t)$ is sketched by plotting it for three values of t. As time proceeds, the peak due to closed orbits extends more and more to larger r; the expected limiting distribution $\hat{P}$ for $t \to \infty$ is a monotonically decreasing function of r with a sharp peak at the origin, very different from the limit distribution for a Gaussian, which is vanishingly small everywhere along the r axis.

Comparing mirror model A with the OV-wind-tree model, one notices that, while both have non-Gaussian $P(\mathbf{r}, t)$, in the former case, $\Delta(t) \sim t$, so that a diffusion coefficient can be defined, while in the latter case $\Delta(t) \sim t^{1-\alpha(n)}$ $[\alpha(n) > 0]$, so that no diffusion coefficient can be defined. An

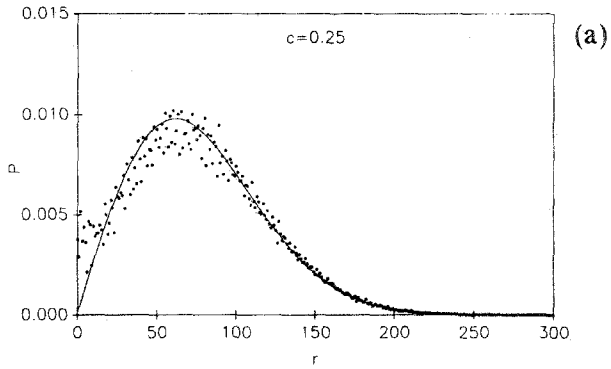

Fig. 9. Probability density distribution functions $\hat{P}$ of the fixed mirror model for four different mirror concentrations at $t = 1024$. The drawn curves are Gaussians with the measured diffusion coefficients. The relative statistical errors are ~ 0.01.

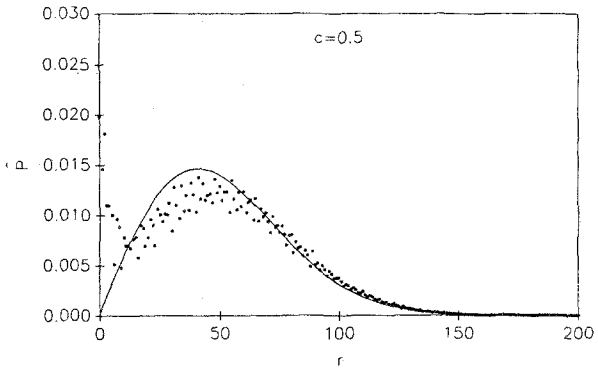

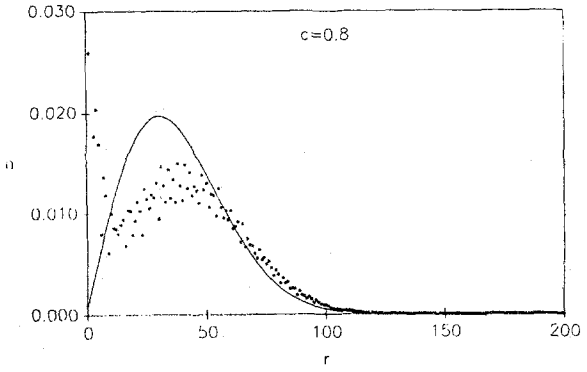

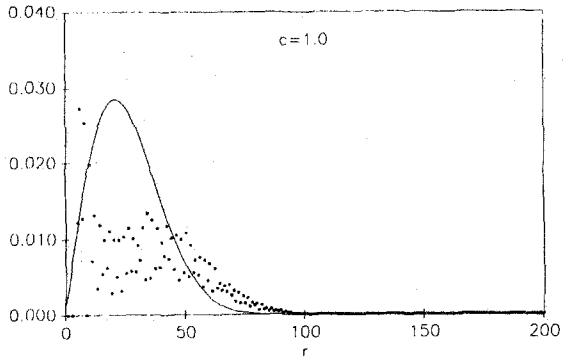

Fig. 9. (*Continued*)

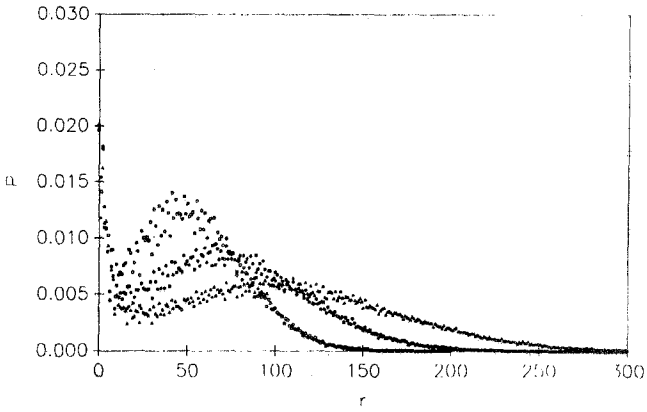

Fig. 10. Probability density distribution functions $\hat{P}$ of the fixed mirror model for $c = 0.5$ at $t = 1024$ (open circles), 2048 (filled circles), and 4096 (filled triangles). The relative statistical errors are ~ 0.01.

important question is: what is the equation that $P(\mathbf{r}, t)$ satisfies? Such an equation would capture mathematically a diffusion process for a deterministic model, incorporating in particular the occurrence of closed orbits.

5.2.2. Model B. (i) Mean square displacement. Again $\Delta(t) \sim t$,[13,14] so that a diffusion coefficient D can be defined; we plot $cD(c)$ versus c for $c_R = c_L$ in Fig. 7. The deviations from the Boltzmann result are small and negative for $c < 0.75$. These negative deviations could well be due to memory effects associated with ring collisions. For $c > 0.75$, the positive

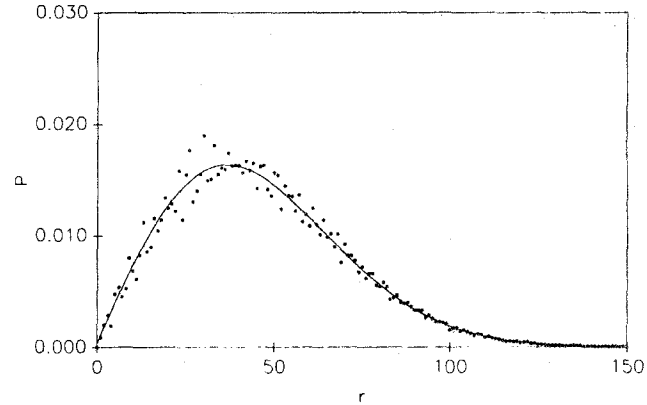

Fig. 11. Probability density distribution function $\hat{P}$ of the flipping mirror model for $c = 1.0$ at $t = 2053$. The drawn curve is a Gaussian with the measured diffusion coefficient. The relative statistical errors are ~ 0.01.

deviations appear to be related to zigzag events.[14] Since these results for D do not change when one puts only one particle on the lattice, no effect of an interaction between the particles due to the flipping of the mirrors is apparent here.

(ii) The kurtosis in this model is zero for all c (cf. Fig. 8), suggesting a normal diffusion process and an absence of closed orbits.

(iii) Indeed, the distribution function $P(\mathbf{r}, t)$ is indistinguishable from that obtained for a Gaussian $P(\mathbf{r}, t)$ and in particular, no peak at the origin occurs (cf. Fig. 11).

6. CONNECTION WITH POLYMER STATISTICS AND PERCOLATION

6.1. Polymer Statistics

It is well known that a self-avoiding walk (SAW) on a lattice can be related to the statistics of polymer chains.[15] A different kind of SAW, the smart kinetic walk (SKW), has been introduced by Weinrib and Trugman[16] on a triangular lattice. The motion of a wind particle on the square lattice for the case $c_L = c_R = 1/2$ of the fixed mirror model can be considered as an SKW. In this walk the wind particle has a probability 1/2 to turn left of right when it visits a lattice site occupied by a mirror for the first time, since there is an equal *a priori* chance that this mirror is a right or a left mirror. However, the probability for the particle to turn left or right upon a second visit to the same mirror is 1, since the particle will remember the fixed orientation of the mirror. This memory constitutes the smartness of the walk and is the difference with the SAW. The walk terminates when the wind particle comes back to its starting point with its initial velocity, so that the length of the walk no longer grows. It has been argued[17] that the SKW can be used to describe the statistics of polymer chains in a solvent at the collapse point, the $T = \Theta$ point. This is the transition point where, with decreasing temperature T, the chain suddenly transforms from an extended to a compact object.

If the interaction energy between nearest neighbor monomers in the polymer chain is J, then the Boltzmann weight for all configurations of a chain with M pairs of interacting monomers contains a factor

$$e^{JM/k_B T} \tag{6.1}$$

Since there is no interaction energy in a SAW, i.e., $J = 0$, all realizations of a SAW of a given total length have the same Boltzmann weight. However, from the construction of our SKW—in particular, that the probability of

turning is equal to 1 instead of 1/2 when the wind particle hits the same mirror for the second time—it follows that its Boltzmann weight is

$$W_{\mathrm{SKW}} = W_{\mathrm{SAW}} 2^M = W_{\mathrm{SAW}} e^{M \ln 2} \tag{6.2}$$

where M is the number of mirrors hit twice by the wind particle. Thus our SKW can be considered to be at a temperature $k_B T = -J/\ln 2$, where J is the attractive nearest neighbor interaction energy. Furthermore, it is unclear[18] whether the SKW on a triangular lattice belongs to the same universality class as a polymer chain at the Θ point, because of the presence of next-nearest-neighbor interactions. Since such interactions are absent in the case of our square lattice, it is reasonable to assume that our SKW is in the same universality class as a polymer chain at its Θ point and is therefore a good model for such a chain at the Θ point.

6.2. Percolation

The right and left mirrors in the fixed mirror model can be mapped onto the bonds of a bond percolation problem on two sublattices of the original lattice (cf. Fig. 12). For the case $c = 1$, when all lattice sites are occupied by mirrors and $c_R = c_L = 1/2$, the probability of occupancy of each bond of each sublattice by a mirror is 1/2. Thus, each sublattice is at the bond percolation threshold,[19] where an infinite cluster of bonds appears. Since any mirror can be on one and only one of the two sub-

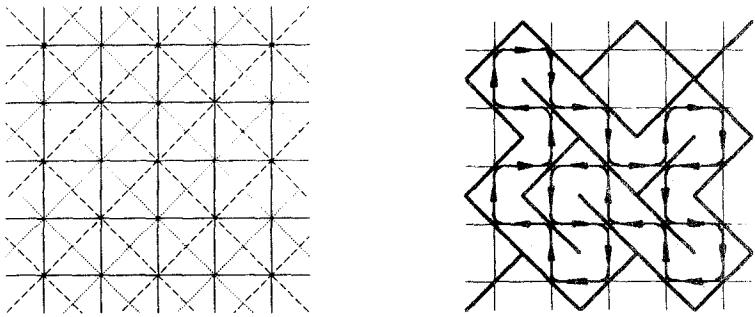

Fig. 12. (a) Two sublattices (dashed and dotted lines); (b) two bond (mirror) clusters, each of which is on one of the two sublattices. Their common boundary is shown to be the trajectory of a moving particle on the original lattice. The number of mirrors hit twice here is $M = 7$.

lattices, the percolation clusters formed by the bonds on the two sublattices are separated and not interconnected. The boundaries of these percolation clusters can be considered as the trajectories of moving particles on the original lattice (cf. Fig. 12).

This connection allows a dynamical calculation of the scaling exponents of the bond percolation problem on the sublattices as well as of those associated with the statistics of polymer chains, through properties of the trajectories of particles on the original lattice.

Thus, the scaling theory result for the square of the end-to-end distance of polymers chains consisting of N monomers,[15,20]

$$\langle r_N^2 \rangle_o \sim N^{2\nu}, \qquad \text{with} \quad \nu = 4/7 \tag{6.3}$$

can be compared with the mean square displacement at time $t = N$, $\Delta_o(t)$, of the—at this time still—open orbits of a wind particle, to which the subscript o refers. We find for $c = 1$ and $t = 10{,}000$, $\nu = 1.141 \pm 0.003$,[14] consistent with (6.3).

Similarly, from percolation theory it follows that the probability for open orbits of length N is given by[21]

$$P_o(N) \sim N^{-1/7} \tag{6.4}$$

which is consistent with our result of an exponent $= -0.142 \pm 0.003$[14] for an open trajectory at time $t = N = 2^{17}$.

7. DISCUSSION

(i) There is a fundamental difference between probabilistic and deterministic lattice gases in that only in the latter can permanently closed orbits, i.e., periodic orbits, occur. For, although a particle can return to its original position and velocity also in a probabilistic gas, at every instant of time there is a finite probability that the particle will jump out of the previously covered part of its trajectory. This "stability" of closed orbits in the deterministic model seems to be at the root of the abnormal diffusion in those models as well as of the mapping—for $c = 1$—onto the polymer statistics problem.

(ii) It would be interesting to extend the present study to triangular lattices, the behavior of which should resemble more the circular Lorentz models. In addition, a study of the mirror model on a cubic lattice would be of interest.

(iii) The occurrence of many closed orbits near the origin in the fixed mirror model implies that a photon beam radiated into the lattice along a

bond at the origin would retain a finite intensity near the origin for all time, trapping a number of photons permanently into closed orbits near the origin. On the contrary, in the flipping mirror model, no such trapping would occur and only a vanishingly small number of photons would remain in time at the origin.

(iv) As mentioned before, it would be of importance to obtain an equation for $P(\mathbf{r}, t)$ for the fixed mirror model. For, such an equation would incorporate the effect of closed orbits in the abnormal diffusion process. It would describe a new type of diffusion, for which the central limit theorem does not hold because of correlations, among others, due to closed orbits. In a more general context, such an equation would contain features that could be relevant not only for the lattice gas diffusion problem considered here, but possibly also for other diffusion processes with deterministic constraints, such as those occurring in polymer diffusion, as discussed by Edwards.[22]

ACKNOWLEDGMENT

This work was performed in part under Department of Energy (DOE) grant DE-FG02-88ER13847.

REFERENCES

1. H. A. Lorentz, *Proc. R. Acad. Amst.* 7:438, 585, 684 (1905).
2. P. Ehrenfest, *Collected Scientific Papers* (North-Holland, Amsterdam, 1959), p. 229.
3. E. G. D. Cohen, in *Théories cinétiques classiques et relativistes* (Proceedings of the Colloques Internationaux du Centre National de la Recherche Scientifique, 1974), M. G. Pichon, ed. (Centre National de la Recherche Scientifique, Paris, 1975), p. 269.
4. E. H. Hauge and E. G. D. Cohen, *J. Math. Phys.* **10**:397 (1969).
5. H. van Beijeren and E. H. Hauge, *Phys. Lett.* **39A**:397 (1972).
6. W. W. Wood and F. Lado, *J. Comp. Phys.* 7:528 (1971).
7. E. H. Hauge, in *Tranaport Phenomena*, G. Kirczenow and J. Marro, eds. (Springer-Verlag, Berlin, 1974), p. 337.
8. S. W. Haan and R. Zwanzig, *J. Phys. A* **10**:1547 (1977).
9. P. M. Binder, *Complex Systems* **1**:559 (1987).
10. M. H. Ernst and P. M. Binder, *J. Stat. Phys.* **51**:981 (1988).
11. M. H. Ernst, G. A. van Velzen, and P. M. Binder, *Phys. Rev. A* **39**:4327 (1989).
12. M. H. Ernst and G. A. van Velzen, *J. Phys. A* (in press).
13. Th. W. Ruijgrok and E. G. D. Cohen, *Phys. Lett. A* **133**:415 (1988).
14. X. P. Kong and E. G. D. Cohen, *Phys. Rev. B* **40**:4838 (1989).
15. P. G. de Gennes, *Scaling Concepts in Polymer Physics* (Cornell University Press, Ithaca, New York, 1979).
16. A. Weinrib and S. A. Trugman, *Phys. Rev. B* **31**:2993 (1985).

17. A. Coniglio, N. Jan, I. Majid, and H. E. Stanley, *Phys. Rev. B* **35**:3617 (1987).
18. P. H. Poole, A. Coniglio, N. Jan, and H. E. Stanley, *Phys. Rev. Lett.* **60**:1203 (1988); *Phys. Rev. B* **39**:495 (1989).
19. D. Stauffer, *Introduction to Percolation Theory* (Taylor and Francis, London, 1985).
20. H. Saleur and B. Duplantier, *Phys. Rev. Lett.* **58**:2325 (1987).
21. R. M. Ziff, *Phys. Rev. Lett.* **56**:454 (1986).
22. S. F. Edwards, *J. Stat. Phys.*, this issue.